

## Synthesis, magnetic and transport properties of La<sub>0.7</sub>Ca<sub>0.15</sub>Sr<sub>0.15</sub>MnO<sub>3</sub> nanoparticles.

S. Punna Rao<sup>1</sup>, K. Suresh Babu<sup>2</sup>

### Abstract

The nanocrystalline La<sub>0.7</sub>Ca<sub>0.15</sub>Sr<sub>0.15</sub>MnO<sub>3</sub> compound have been synthesized by combustion method. X-ray diffraction of prepared samples crystallize in the rhombohedral ( $R\bar{3}c$ ) structure. The crystallite size increases with increasing annealing temperature. The magnetization data reveals the distinct suppression  $T_C$  i. e. the ferromagnetic (FM) to paramagnetic (PM) transition with decreasing crystallite size. The transport properties show that the metal-insulator ( $T_{MI}$ ) transition decreased and resistivity increases with decreasing crystallite size. The observed results are explained terms of the surface disorder and opening of strong AFM coupling at the expense of FM ordering in the nano crystallites of La<sub>0.7</sub>Ca<sub>0.15</sub>Sr<sub>0.15</sub>MnO<sub>3</sub> system.

**Keywords:** Nanocrystallites, Metal-insulator transition, Ferromagnetic transition, Coercivity, Surface disorder.

### 1. Introduction

R<sub>1-x</sub>A<sub>x</sub>MnO<sub>3</sub> (R - rare-earth ions and A - divalent alkaline-earth metal ions) in the form of nanocrystalline are very important in technological applications because of their colossal magnetoresistance (CMR) effects.

Lanthanum manganites compounds are studied extensively to optimize the Curie temperature and magnetoresistance (MR). These compounds exhibits a well known bell shape with radius [1-4]. If A site is doped with Ca the maximum MR is observed, whereas if Sr was doped at A site the MR value is low. If double doping (Ca and Sr), La<sub>0.7</sub>Ca<sub>0.3-x</sub>Sr<sub>x</sub>MnO<sub>3</sub> it undergoes a structural transition [5-8]. This transition is influenced by external perturbation of the crystal lattice (such as lattice strain) [6]. It is worthwhile to investigate the influence of the crystallite size without disturbing  $r_A$  in the vicinity of above noted structural and ferromagnetic phase transition. The magnetic and electric transport properties of nano scale manganites are differ significantly from the bulk [9-12]. There has been no report on the effect of crystallite size in La<sub>0.7</sub>Ca<sub>0.15</sub>Sr<sub>0.15</sub>MnO<sub>3</sub> compound. In this manuscript we study the influence of crystallite size on structural, magnetic, and transport properties of La<sub>0.7</sub>Ca<sub>0.15</sub>Sr<sub>0.15</sub>MnO<sub>3</sub> compound.

### 2. Experimental details

Nanocrystallites of nominal composition La<sub>0.7</sub>Ca<sub>0.15</sub>Sr<sub>0.15</sub>MnO<sub>3</sub> were synthesized by combustion method. The materials used in the synthesis were metal nitrates: La(NO<sub>3</sub>)<sub>3</sub>·6H<sub>2</sub>O, Sr(NO<sub>3</sub>)<sub>2</sub>, Mn(NO<sub>3</sub>)<sub>2</sub>·6H<sub>2</sub>O, Ca(NO<sub>3</sub>)<sub>2</sub>·4H<sub>2</sub>O, and the propellants were urea and citric acid. The

---

<sup>1</sup>Faculty of Pharmacy, Lincoln University College, Malaysia

<sup>2</sup>Corresponding Author: K. Suresh Babu & babuiict@gmail.com

samples were synthesized by combustion method, using urea and citric acid as fuel agents. The metal nitrates were dissolved with the fuel (fuel/metal nitrates ratio was 1:2) in distilled water and heated (under stirring) at  $80^\circ\text{C}$ , until the water evaporation and formation of a gel. After that, the gel was heated at  $300^\circ\text{C}$ . Once ignited, the gel underwent a combustion process and yielded a voluminous powder. The powder was separated into different parts and calcined for 6 h in air at different temperatures such as  $600$ ,  $1000$ , and  $1250^\circ\text{C}$ .

The structure and phase purity of the samples were checked by powder X-ray diffraction (XRD) using the  $\text{Cu-K}\alpha$  radiation at room temperature. The field cooled (FC) and zero field cooled (ZFC) magnetization curves were measured in a commercial SQUID magnetometer with the temperature range from  $4$  K to  $400$  K in an applied field of  $50$  Oe and  $1$  kOe, and the hysteresis curves were measured at  $10$  K for  $-50$  kOe  $\leq H \leq +50$  kOe. The dc resistivity of the samples were measured using the conventional four-probe method in the temperature range from  $10$  K to  $350$  K in a closed cycle helium refrigerator.

### 3. Results and discussion

Figure 1 shows the X-ray diffraction patterns of the  $\text{La}_{0.7}\text{Ca}_{0.15}\text{Sr}_{0.15}\text{MnO}_3$  nanocrystallites. XRD pattern of all these crystallites can be indexed by a rhombohedral structure with space group  $R\bar{3}c$  [13,14]. The average crystallite size ( $d$ ) of the nanocrystallite of  $\text{La}_{0.7}\text{Ca}_{0.15}\text{Sr}_{0.15}\text{MnO}_3$  was evaluated by using the Debye-Scherrer's equation: equation:  $d = 0.9\lambda / (\beta \cos\theta)$ , where  $\lambda$  is the wavelength of  $\text{Cu K}\alpha$  radiation ( $\lambda = 1.5406$  Å),  $\beta$  is the full width at half maximum intensity (FWHM) of strong peak, and  $\theta$  is the corresponding diffraction angle. The average crystallite sizes were found to be  $14$ ,  $43$ , and  $58$  nm for the  $\text{La}_{0.7}\text{Ca}_{0.15}\text{Sr}_{0.15}\text{MnO}_3$  nanocrystallites post-annealed at  $600$ ,  $1000$ , and  $1250^\circ\text{C}$ , as indicated in Fig. 1.

The temperature dependent magnetization ( $M$ ) for different sizes of  $\text{La}_{0.7}\text{Ca}_{0.15}\text{Sr}_{0.15}\text{MnO}_3$  nanocrystallites in a field of  $H = 1$  kOe are shown in figure 2. The nearly temperature independent behavior observed in the  $M(T)$  curves at low temperature indicates that the long range FM ordering persists for all nanocrystallites. A sharp transition from a PM to a FM state is observed for crystallite size greater than  $43$  nm. For crystallite size of  $58$  nm, the obtained value of the  $T_C$  is  $\sim 350$  K, consistent with previous reports [6]. The  $T_C$  defined as the temperature corresponding to the maximum of  $-dM/dT$  in the  $M(T)$  curve. It is observed that the  $T_C$  decreases monotonically with increasing crystallite size, where  $T_C$  of  $\sim 275$  K is observed for the crystallite size of  $14$  nm.

Figure 3 shows the typical field dependence of magnetization for different sizes of  $\text{La}_{0.7}\text{Ca}_{0.15}\text{Sr}_{0.15}\text{MnO}_3$  nanocrystallites at  $10$  K. The magnetization tends to saturate at low fields for all the crystallite sizes, indicating a long-range FM order. The saturation magnetic moment decreases with reducing crystallite size (Figure 4) which may be attributed to increase in the number of grain boundaries and the surface effects. The remnant magnetization ( $M_r$ ) and coercive fields ( $H_c$ ), increases with the decrease in crystallite size (Figure 4). The higher value of the coercivity for the small nanocrystallites indicates that the presence of dead layer with random spin orientation and thickness of dead layer increases with the decrease in crystallite size [15]. The variation in magnetic properties with crystallite size can be explained by using the core-shell model [16]. It has been reported earlier that a few nanometers thick layer ( $1-5$  nm) is present on the crystallite (shell), which is anti-ferromagnetic or amorphous in nature and core of the nanocrystallites behaves as a bulk material. As the crystallite size decreases the thickness of the shell increases and the inter-core separation increases, which results in the decrease in saturation magnetization and increase in the values of coercivity and remanent magnetization with

crystallite size.

The temperature dependence of resistivity  $\rho(T)$  curves for the different sizes of  $\text{La}_{0.7}\text{Ca}_{0.15}\text{Sr}_{0.15}\text{MnO}_3$  nanocrystallites measured at zero field are plotted in figure 5-7. The  $\rho(T)$  curve of 58 nm size crystallites shows a single metal insulator transition  $T_{\text{IM}}$  at 328 K (figure 7), which is less than the magnetic transition  $T_{\text{C}}$ . The value of  $T_{\text{IM}}$  decreases drastically with decreasing crystallite size, where  $T_{\text{IM}}$  of  $\sim 225$  K is observed for the crystallite size of 14 nm (figure 6). With increasing crystallite size lowers the resistivity. In nanocrystalline samples charge carriers are scattered at grain boundaries. As the crystallite size in a sample decreases the number of grain boundaries increases resulting in the scattering of more number of charge carriers which thereby increases the resistivity [17]. When an external magnetic field is applied, decrease in the value of resistivity for all the samples at all temperatures was observed (not shown here). When magnetic field is applied the spin ordering increases and the localization of the charge decreases, which may result in the reduction of resistivity in the presence of magnetic field [18]. The temperature dependent resistivity has three different regions related to the different conduction mechanism involved at different temperatures.

#### 4. Conclusions

We have studied the effect of crystallite size on structure, magnetic, and magneto transport properties in  $\text{La}_{0.7}\text{Ca}_{0.15}\text{Sr}_{0.15}\text{MnO}_3$  nanocrystallites. Powder x-ray analysis reveals that the nanocrystallites undergoes rhombohedral structure. The temperature dependent magnetization  $M(T)$  data reveal that an increase in magnetization and decrease in coercivity with increase in crystallite size. The resistivity  $\rho(T)$  curves show that the metal insulator transition value of  $T_{\text{IM}}$  decreases drastically and increasing resistivity with decreasing crystallite size. As the crystallite size in a sample decreases the number of grain boundaries increases resulting in the scattering of more number of charge carriers which is responsible for the above results. The present results suggest that varying transition temperature could be a potential way in tuning CMR at room temperature.

#### References

- [1] von Helmolt R, Wecker J, Holzapfel B, Schultz L and Samwer K 1993 *Phys. Rev. Lett.* **71** 2331
- [2] M. Imada M, Fujimori A and Tokura Y 1998 *Rev. Mod. Phys.* **70** 1039
- [3] Rao C N R and Raveau B (ed) 1998 *Colossal Magneto resistance, Charge Ordering, and Related Properties of Manganese Oxides* (World Scientific, Singapore); Tokura Y (ed) 2000 *Colossal Magnetoresistive Materials* (Gordon & Breach, New York)
- [4] Hwang H Y, Cheong S -W, Radaelli P G, Marezio M and Batlogg B 1995 *Phys. Rev. Lett.* **75** 914
- [5] Radaelli P G, Marezio M, Hwang H Y, Cheong S -W and Batlogg B 1996 *Phys. Rev. B* **54** 8992
- [6] Tomioka Y, Asamitsu A and Tokura Y 2000 *Phys. Rev. B* **63** 024421
- [7] Mira J, Rivas J, Hueso L E, Rivadulla F, Lopez Quintela M A, Senaris Rodriguez M A and Ramos C A 2002 *Phys. Rev. B* **65** 024418
- [8] Ulyanov A N, Yu S C, Yu Starostyuk N, Pismenova N E, Moon Y M and Lee K W 2002 *J. Appl. Phys.* **90** 8900
- [9] Dey P and Nath T K 2006 *Phys. Rev. B* **73** 214425
- [10] Lopez-Quintela M A, Hueso L E, Rivas J and Rivadulla F 2003 *Nanotechnology* **14** 212

## Synthesis, magnetic and transport properties of $\text{La}_{0.7}\text{Ca}_{0.15}\text{Sr}_{0.15}\text{MnO}_3$ nanoparticles.

- [11] Shantha K, Shankar Kar S, Subbanna G N and Raychaudhuri A K 2004 *Solid State Commun.* **129** 479
- [12] Navin, K and Kurchania, R. 2020 *Appl. Phys. A* **126**, 100
- [13] Joint Committee on Powder Diffraction Standards, Powder Diffraction Files, Card No. 30-1287
- [14] Shannon R D and Prewitt C T 1976 *Acta Crystallogr. Sect. A Cryst. Phys., Diffr., Theor. Gen. Crystallogr.* **32** 785
- [15] Baaziz H, Tozri A, Dhahri E, Hlil E K 2005 *Ceram. Int.* **41** 2955
- [16] Curiale J, Granada M, Troiani H, Sánchez R, Leyva A, Levy P, Samwer K 2009 *Appl. Phys. Lett.* **95**, 043106
- [17] Andres A, Gracia-Hernandez M, Martinez J, 1999 *Phys. Rev. B* **60** 7328.
- [18] Hwang H Y, Cheong S W, Ong N P, Batlogg B 1996 *Phys. Rev. Lett.* **77** 2041.

### Figure Captions

Figure 1 The room temperature XRD spectra of nanocrystalline  $\text{La}_{0.7}\text{Ca}_{0.15}\text{Sr}_{0.15}\text{MnO}_3$  samples.

Figure 2. The temperature dependent magnetization (M) for different sizes of  $\text{La}_{0.7}\text{Ca}_{0.15}\text{Sr}_{0.15}\text{MnO}_3$  nanocrystallites.

Figure 3. The magnetic hysteresis M (H) curves for different sizes of  $\text{La}_{0.7}\text{Ca}_{0.15}\text{Sr}_{0.15}\text{MnO}_3$  nanocrystallites measured at 10 K.

Figure 4. The low field magnetic hysteresis M (H) curves for different sizes of  $\text{La}_{0.7}\text{Ca}_{0.15}\text{Sr}_{0.15}\text{MnO}_3$  nanocrystallites measured at 10 K.

Figure 5. The temperature dependence of resistivity  $\rho(T)$  curves for 14 nm crystallite size of  $\text{La}_{0.7}\text{Ca}_{0.15}\text{Sr}_{0.15}\text{MnO}_3$  measured at zero field.

Figure 6. The temperature dependence of resistivity  $\rho(T)$  curves for 43 nm crystallite size of  $\text{La}_{0.7}\text{Ca}_{0.15}\text{Sr}_{0.15}\text{MnO}_3$  measured at zero field.

Figure 7. The temperature dependence of resistivity  $\rho(T)$  curves for 58 nm crystallite size of  $\text{La}_{0.7}\text{Ca}_{0.15}\text{Sr}_{0.15}\text{MnO}_3$  measured at zero field.

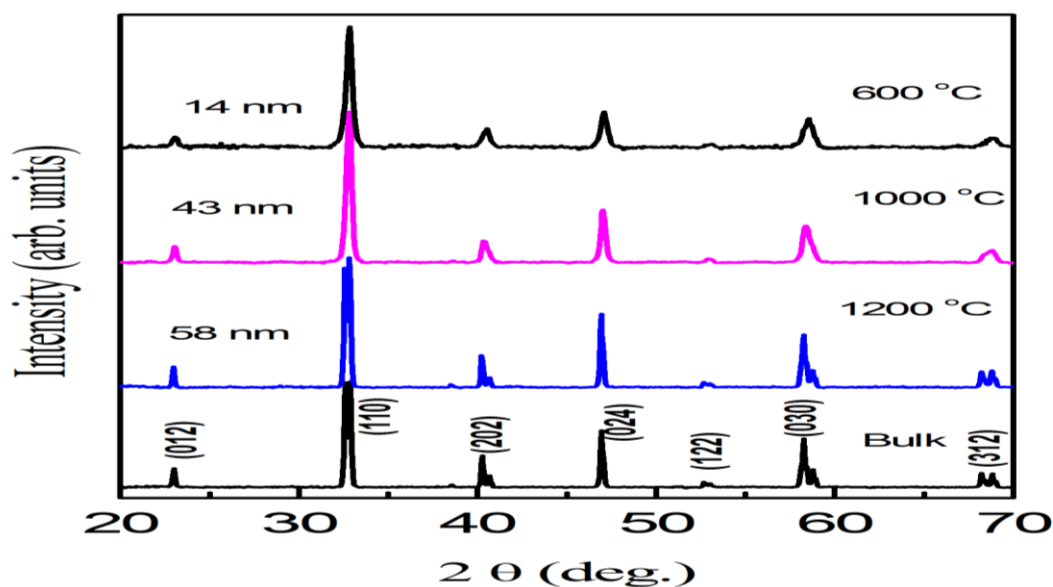


Fig. 1

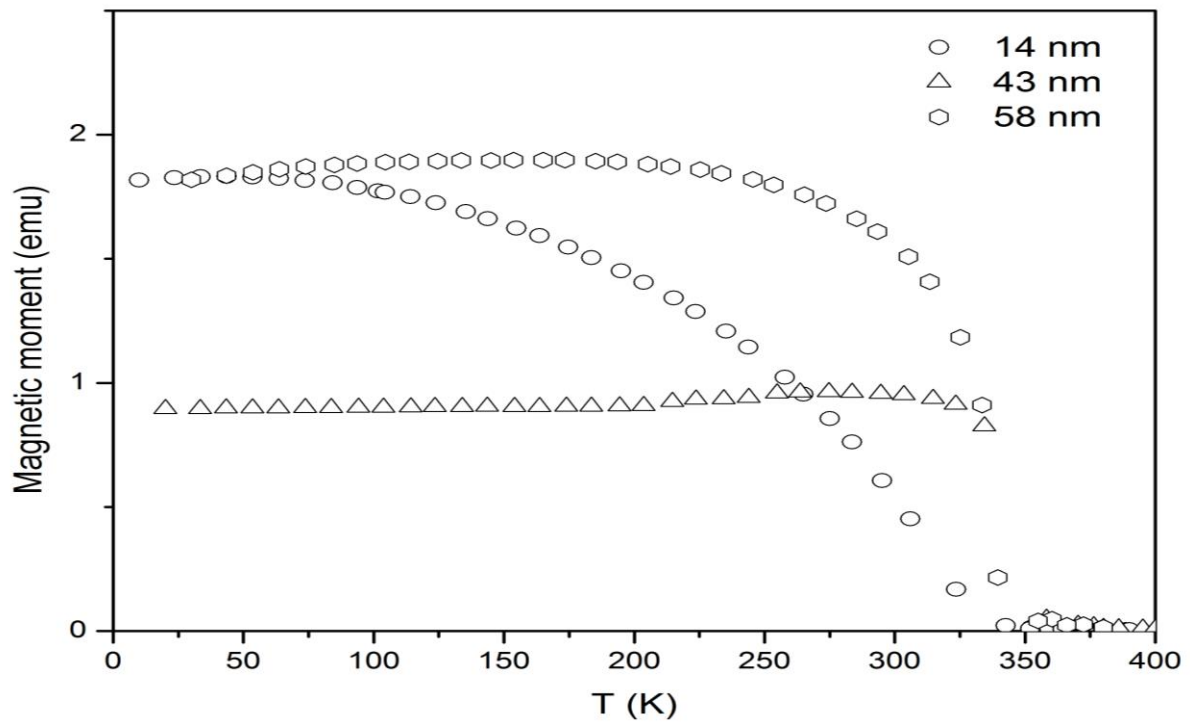


Fig. 2

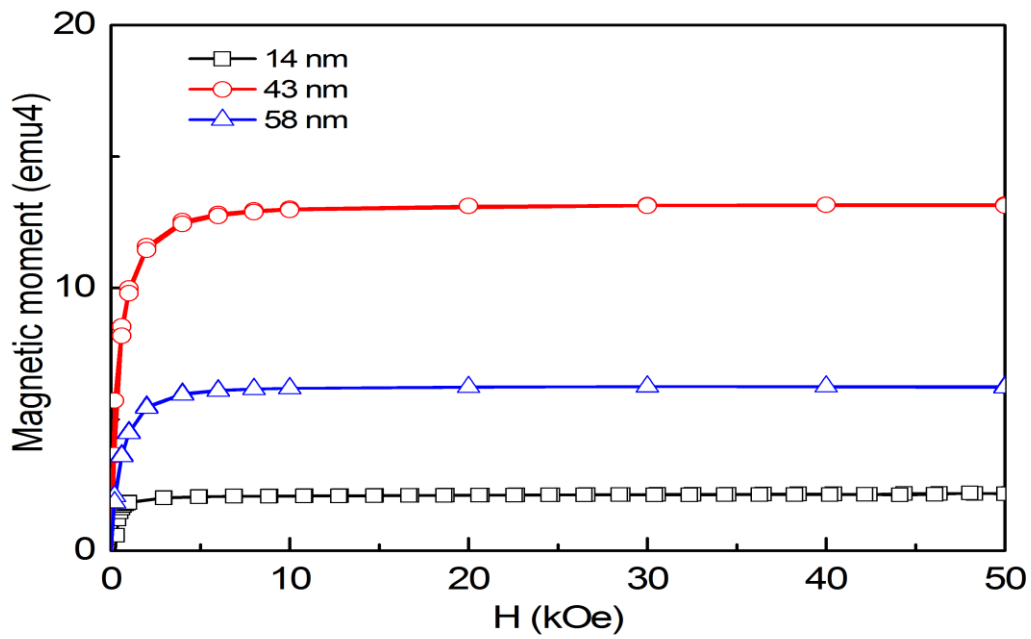


Fig. 3

Synthesis, magnetic and transport properties of  $\text{La}_{0.7}\text{Ca}_{0.15}\text{Sr}_{0.15}\text{MnO}_3$  nanoparticles.

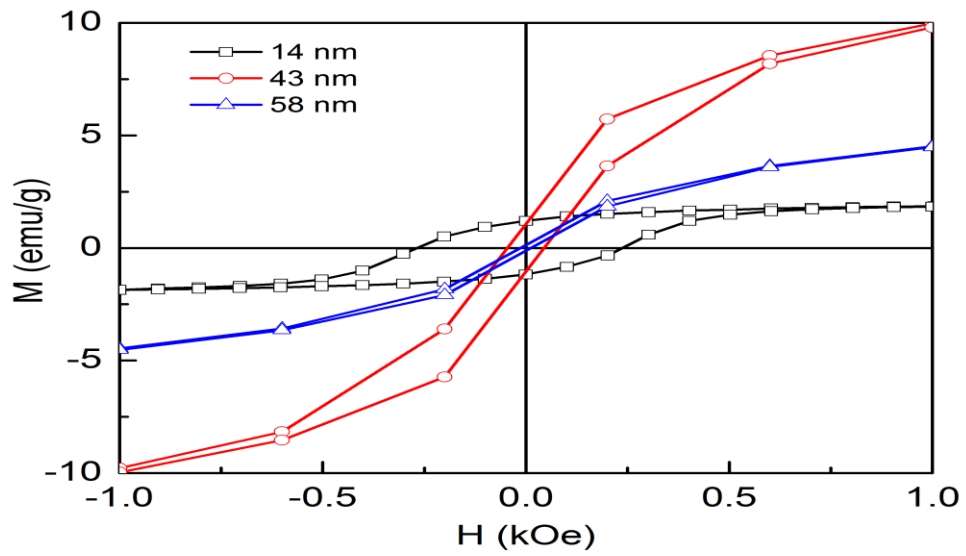


Fig. 4

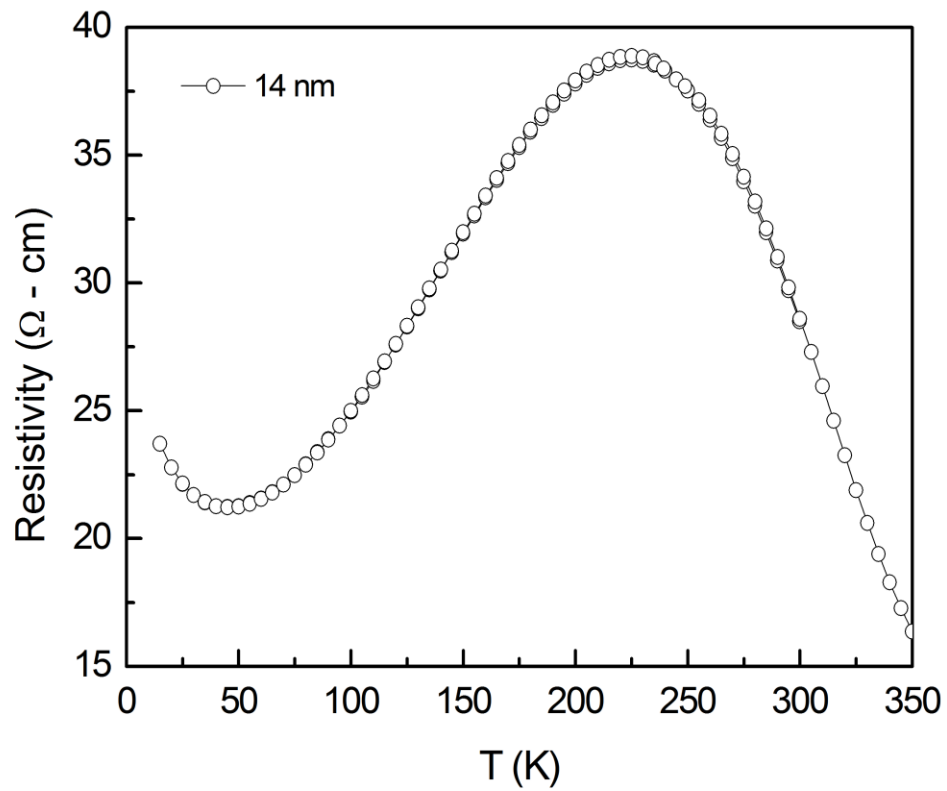


Fig. 5

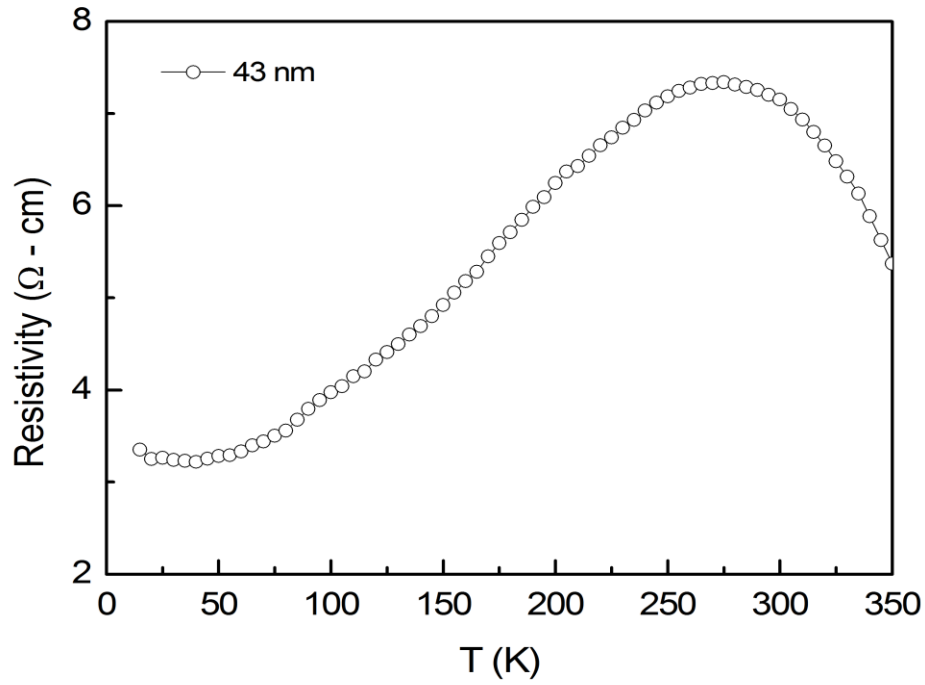


Figure 6

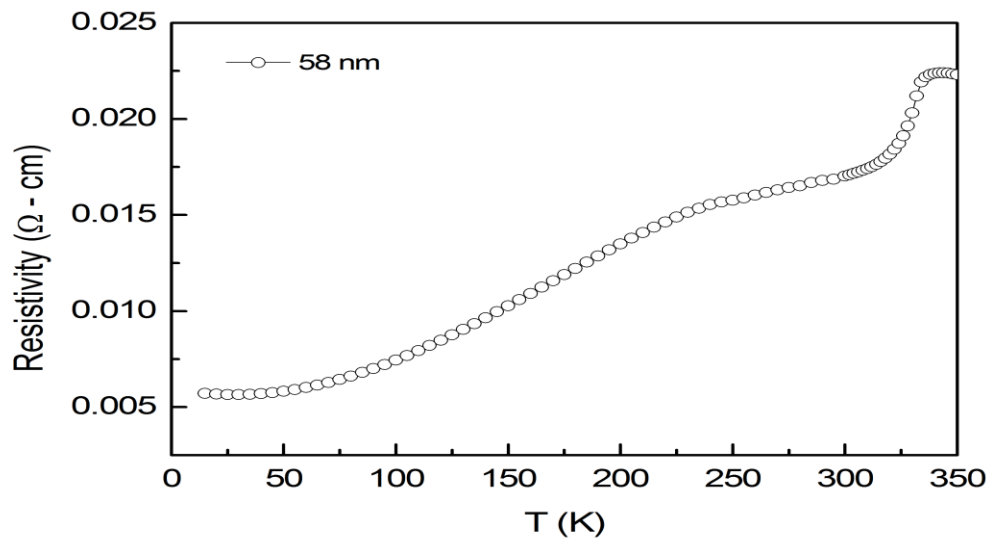


Figure 7